

Research Space

Journal article

Differential nucleosome occupancy modulates alternative splicing in *Arabidopsis thaliana*

**Jabre, I., Chaudhary, S., Guo, W., Kalyna, M., Reddy, A. S. N.,
Chen, W., Zhang, R., Wilson, C. and Syed, N.**

*"This is the peer reviewed version of the following article: Jabre, I., Chaudhary, S., Guo, W., Kalyna, M., Reddy, A.S.N., Chen, W., Zhang, R., Wilson, C. and Syed, N.H. (2020), Differential nucleosome occupancy modulates alternative splicing in *Arabidopsis thaliana*. New Phytologist. Accepted Author Manuscript. <https://doi.org/10.1111/nph.17062>, which has been published in final form at <https://doi.org/10.1111/nph.17062>. This article may be used for non-commercial purposes in accordance with Wiley Terms and Conditions for Use of Self-Archived Versions."*



New Phytologist

Differential nucleosome occupancy modulates alternative splicing in *Arabidopsis thaliana*

Journal:	<i>New Phytologist</i>
Manuscript ID	NPH-RAP-2020-34391.R1
Manuscript Type:	RAP - Rapid Report
Date Submitted by the Author:	n/a
Complete List of Authors:	Jabre, Ibtissam ; Canterbury Christ Church University, Human and Life Sciences Chaudhary, Saurabh; Cardiff University, School of Biosciences Guo, Wenbin; The James Hutton Institute, Informatics and Computational Sciences Kalyna, Maria; University of Natural Resources and Life Sciences, Department of Applied Genetics and Cell Biology REddy, Anireddy; Colorado State University, Department of Biology and Program in Cell and Molecular Biology Chen, Weizhong; Cornell University, Department of Molecular Biology and Genetics Zhang, Runxuan; James Hutton Institute, Informatics and Computational Sciences; The James Hutton Institute Wilson, Cornelia; Canterbury Christ Church University, Human and Life Sciences Syed, Naeem; Canterbury Christ Church University, Human and Life Sciences;
Key Words:	Alternative Splicing, Cold Stress, Nucleosome Positioning, Exons, Co-transcriptional Splicing, <i>Arabidopsis thaliana</i>

SCHOLARONE™
Manuscripts

1 **Differential nucleosome occupancy modulates alternative splicing in**
2 ***Arabidopsis thaliana***

3

4 Ibtissam Jabre^{1*6}, Saurabh Chaudhary^{1*7}, Wenbin Guo³, Maria Kalyna², Anireddy S N Reddy⁴,
5 Weizhong Chen⁵, Runxuan Zhang³, Cornelia Wilson¹ and Naeem H Syed¹

6

7 ¹School of Human and Life Sciences, Canterbury Christ Church University, Canterbury, CT1
8 1QU, UK.

9 ²Department of Applied Genetics and Cell Biology, University of Natural Resources and Life
10 Sciences - BOKU, Muthgasse 18, 1190 Vienna, Austria.

11 ³Computational Sciences, The James Hutton Institute, Dundee DD2 5DA, UK.

12 ⁴Department of Biology and Program in Cell and Molecular Biology, Colorado State
13 University, Fort Collins, CO 80523-1878, USA.

14 ⁵Department of Molecular Biology & Genetics, Cornell University, Ithaca, NY 14853-2703,
15 USA.

16 ⁶School of Biosciences and Medicine, University of Surrey, Guildford GU2 7XH, UK.

17 ⁷Cardiff School of Biosciences, Cardiff University, Cardiff, CF10 3AX, UK.

18

19 *Contributed equally

20 Corresponding author: Naeem Syed, Canterbury Christ Church University, Canterbury, CT1
21 1QU; phone +44 1227 782511; Email: naeem.syed@canterbury.ac.uk

22

23

24 **Introduction:** 618 words

25 **Materials and Methods:** 297 words

26 **Results:** 1424 words

27 **Discussion:** 806 words

28 **Figures:** Four coloured

29 **Tables:** NIL

30 **Supporting Information:** Nine files

31

32

33 **Summary**

- 34 • Alternative splicing (AS) is a major gene regulatory mechanism in plants. Recent
35 evidence supports co-transcriptional splicing in plants, hence the chromatin state can
36 impact AS. However, how dynamic changes in the chromatin state such as nucleosome
37 occupancy influence the cold-induced AS remains poorly understood.
- 38 • Here, we generated transcriptome (RNA-Seq) and nucleosome positioning (MNase-
39 Seq) data for *Arabidopsis thaliana* to understand how nucleosome positioning
40 modulates cold-induced AS.
- 41 • Our results show that characteristic nucleosome occupancy levels are strongly
42 associated with the type and abundance of various AS events under normal and cold
43 temperature conditions in Arabidopsis. Intriguingly, exons, alternatively spliced
44 internal regions of protein-coding exons, exhibit distinctive nucleosome positioning
45 pattern compared to other alternatively spliced regions. Likewise, nucleosome patterns
46 differ between exons and retained introns pointing to their distinct regulation.
- 47 • Collectively, our data show that characteristic changes in nucleosome positioning
48 modulate AS in plants in response to cold.

49 **Key words:** Alternative Splicing, *Arabidopsis thaliana*, Cold Stress, Co-transcriptional
50 Splicing, Exons, Nucleosome Positioning.

51

52

53

55 Introduction

56 Plants employ different strategies to control their transcriptional program during the daily
57 cycles of light-dark and in response to environmental stress to confer adaptive responses (Zhu,
58 2016; Laloum *et al.*, 2017; Lämke & Bäurle, 2017). Recent evidence shows that alternative
59 splicing (AS) regulation is a key gene regulatory mechanism in plants (Calixto *et al.*, 2018;
60 Filichkin *et al.*, 2018; Jabre *et al.*, 2019). In plants and animals, AS is regulated co-
61 transcriptionally (Brody *et al.*, 2011; Tilgner *et al.*, 2012; Li *et al.*, 2020; Zhu *et al.*, 2020).
62 RNA polymerase II (RNAPII) speed during transcription may be affected by the chromatin
63 state that in turn determines AS outcomes (Alexander *et al.*, 2010; Ullah *et al.*, 2018; Zhu *et al.*,
64 2018). Emerging evidence shows that the chromatin environment has a strong bearing on
65 the splicing process by modulating RNAPII processivity and splicing factors (SFs) recruitment
66 (Nojima *et al.*, 2018; Jabre *et al.*, 2019; Kindgren *et al.*, 2019; Li *et al.*, 2020; Yu *et al.*, 2019;
67 Zhu *et al.*, 2020). Recent native elongating transcript sequencing (NET-Seq) and global run-
68 on sequencing (GRO-Seq) studies from mammals and *Arabidopsis thaliana* (hereafter
69 *Arabidopsis*) show that phosphorylation of RNAPII C-terminal domain mediates interactions
70 with the spliceosome and that RNAPII accumulation is associated with different chromatin
71 states (Nojima *et al.*, 2018; Zhu *et al.*, 2018). Remarkably, sequencing of the chromatin-bound
72 nascent RNAs in *Arabidopsis* revealed that almost all introns are spliced co-transcriptionally
73 and the efficiency of intron removal is more robust in protein-coding genes than noncoding
74 RNAs (Li *et al.*, 2020). Furthermore, it was also demonstrated that co-transcriptional splicing
75 (CTS) efficiency is dependent on the number of exons but not gene length (Zhu *et al.*, 2020).
76 Therefore, appropriate exon-intron definition may be important for CTS in *Arabidopsis* (Li *et al.*,
77 2020). For example, nucleosome occupancy was found to be higher on exons and also
78 accompanied by a higher level of RNAPII (Chodavarapu *et al.*, 2010). Therefore, higher
79 nucleosome occupancy on exons is intrinsically associated with exon definition, RNAPII
80 processivity and splicing kinetics (Jabre *et al.*, 2019). Previously, it has been demonstrated that
81 change in RNAPII speed in both directions can influence splicing factor recruitment and
82 splicing efficiency (Dujardin *et al.*, 2014; Godoy Herz *et al.*, 2019; Leng *et al.*, 2020).
83 Therefore, nucleosome positioning may modulate different AS events and their ratios under
84 variable growth and/or stress conditions to alter intron/exon boundaries and provide a context
85 through which AS patterns could be modulated (Jabre *et al.*, 2019). For example, RNAi lines
86 of a chromatin remodeler gene (*ZmCHB101*) in maize showed altered nucleosome density,
87 RNAPII elongation rate, and changes in splicing patterns under osmotic stress (Yu *et al.*, 2019).

88 Similarly, widespread nucleosome remodelling in rice, as a result of phosphate starvation and
89 cold stress, was associated with differential gene expression (Roy *et al.*, 2014; Zhang *et al.*,
90 2018). Since cold can influence the RNAPII elongation kinetics in Arabidopsis (Kindgren *et*
91 *al.*, 2019), we reasoned that rapid cold-induced alternative splicing response in Arabidopsis
92 (Calixto *et al.*, 2018) may be associated with nucleosome remodelling. Henceforth, we used
93 cold treatment as a system of choice to investigate whether it could modulate nucleosome
94 positioning and influence AS.

95 We performed RNA-Seq and micrococcal nuclease sequencing (MNase-Seq) for Columbia
96 wild type (Col-0) accession of Arabidopsis growing at normal temperature (22°C) and under
97 cold stress (4°C) for 24 hours. We observed genome-wide changes in AS and gene expression
98 between Col-0_22°C and Col-0_4°C plants. Our results show that temperature-dependent
99 differences in nucleosome positioning are sufficient to modulate different types of AS events
100 and their abundance. Remarkably, exons, alternatively spliced internal regions of protein-
101 coding exons (Marquez *et al.*, 2015), can also be distinguished from flanking exons by
102 distinctive nucleosome occupancy to facilitate their recognition by the splicing machinery.

103

104 **Materials and Methods**

105 The detailed experimental procedure is provided in the supplementary information file
106 (Supporting Information Method S1). Briefly, leaf tissues were harvested from three weeks old
107 Col-0 plants grown at 22°C and cold treated (4°C) for 24 h. Total RNA and nucleosome bound
108 genomic DNA (gDNA) were extracted for Illumina paired-end sequencing using RNA
109 extraction and Qiagen DNA kits, respectively. The raw reads generated from RNA-Seq and
110 MNase-Seq experiments were quality checked using Trimmomatic (Bolger *et al.*, 2014). The
111 high quality reads from RNA-Seq experiment were used to quantify the transcripts expression
112 using Salmon v0.82 (Patro *et al.*, 2017) and AtRTD2-QUASI (Zhang *et al.*, 2017) as reference.
113 Differential Expressed Genes (DEGs) and differential alternatively spliced (DAS) genes were
114 identified using 3D-RNA-Seq pipeline as described previously by (Calixto *et al.*, 2018; Guo *et*
115 *al.*, 2019). Gene functional enrichment analysis was performed using DAVID v6.8 (Huang *et*
116 *al.*, 2009a,b). The gene ontology (GO) terms were assigned to DEGs and DAS genes with FDR
117 ≤ 0.05 . AS events, AS event inclusion level (Percent Spliced In – PSI indicates how efficiently
118 sequences of interest are spliced into transcripts) and the difference in this inclusion (Δ PSI)
119 between Col-0 grown at 22°C and 4°C were identified using SUPPA2 (Alamancos *et al.*, 2015;
120 Trincado *et al.*, 2018). Only AS events having a p -value ≤ 0.05 are identified as DAS events.

121 For MNase-Seq high quality reads were mapped to the TAIR10 Arabidopsis reference genome
122 using Bowtie v1.2.2 (Langmead *et al.*, 2009) with "-m" set to 1 to output only uniquely mapped
123 reads. Improved Nucleosome-Positioning Algorithm (iNPS) was used for accurate genome-
124 wide nucleosome positioning as described previously by (Chen *et al.*, 2014). Differential
125 Nucleosome Positioning (DNP) analysis was performed using DANPOS v2.1.2 (Chen *et al.*,
126 2013). Nucleosome signals were plotted around different genomic regions using deepTools
127 v3.5.0 (Ramírez *et al.*, 2014).

128

129 **Results**

130 **Cold-regulated DE and DAS genes affect different biological processes**

131 In Arabidopsis, nucleosome positioning differentially marks promoter regions, gene bodies as
132 well as exons and introns, indicating a potential link of chromatin architecture to gene
133 expression and splicing regulation (Chodavarapu *et al.*, 2010). To investigate if cold-induced
134 AS in Arabidopsis is regulated by nucleosome occupancy, we performed RNA-Seq and
135 MNase-Seq of Col-0 lines before and after a shift from 22°C to 4°C for 24 hours. Using the
136 previously published 3D-RNA-Seq pipeline (Calixto *et al.*, 2018; Guo *et al.*, 2019) (Supporting
137 Information Method S1), we identified 6252 DEGs and 2283 DAS genes. Of the 6252 DEGs,
138 3323 were up-regulated and 2929 were down-regulated (Table S1). We observed that most
139 transcriptional changes are associated with genes that do not display splicing changes (70.5%
140 DE only genes). Similarly, a large proportion of splicing changes occur in genes that are not
141 differentially expressed (19.3% DAS only genes). The overlap of DEGs and DAS genes is
142 significant (10.2%; hypergeometric test, $p < 1.222e^{-39}$) (Fig. 1a), suggesting that cold stress
143 modulates both transcriptional and AS responses of some genes, which is in line with
144 previously published reports from Arabidopsis (Calixto *et al.*, 2018). Gene functional
145 enrichment analysis of DEGs showed significant (FDR <0.05) enrichment in diverse biological
146 functions including circadian rhythm, cold stress, and photosynthesis regulation. Cellular
147 components terms enrichment for DEGs were mainly for plasma membrane, and vacuole (Fig.
148 S1a). DAS genes showed significant (FDR <0.05) enrichment in mRNA processing, RNA
149 splicing and protein phosphorylation, whereas those of cellular components and molecular
150 functions were mainly enriched in the nucleus and mRNA/ATP/protein binding activities,
151 respectively (Fig. S1b). To identify AS events regulated by cold stress, we analysed RNA-Seq
152 data using SUPPA2 (Supporting Information Method S1) (Alamancos *et al.*, 2015; Trincado *et*

153 *al.*, 2018). We identified 3032 cold-regulated AS events that showed significant (p -value
 154 <0.05) changes in the Δ PSI index (see Methods) distributed within different types of AS events.
 155 Changes in intron retention (IR) events are the most prevalent, followed by usage of alternative
 156 acceptor (A3'SS) and alternative donor (A5'SS) sites, exon skipping (ES), and exitrons (EIs)
 157 (Table S2, S3; Fig. 1b; Fig. S2). EIs are alternatively spliced internal regions of protein-coding
 158 exons (Marquez *et al.*, 2015; Staiger & Simpson, 2015; Sibley *et al.*, 2016). At least 6.6% of
 159 Arabidopsis and 3.7% of human protein-coding genes contain exitrons (Marquez *et al.*, 2015;
 160 Zhang *et al.*, 2017). Due to their distinctive features, we grouped EIs separately from IR events.

161 Nucleosome occupancy modulates variety and abundance of alternative splicing 162 events

163 To investigate how nucleosome occupancy modulates splicing, we performed nucleosome
 164 positioning and DNP analysis (Supporting Information Method S1). We detected 19233
 165 significant Differential Positioned Nucleosomes (DPNs) upon shifting plants from 22°C to 4°C
 166 for 24 hours that were significantly (Supporting Information Method S1) associated with 7357
 167 genes (Tables S4, S5, and S6). Interestingly, 833 (9.5%) (hypergeometric test, $p < 1.498e^{-24}$)
 168 cold-induced DAS genes displayed changes in nucleosome occupancy (Fig. 1c). We first
 169 profiled nucleosome occupancy across exons and flanking regions, where we could detect a
 170 significant drop of nucleosome occupancy signals at 4°C around exons and flanking regions
 171 (one-tailed t test, $p < 0.0001$) (Fig. S3). Then, we sought if changes in nucleosome occupancy
 172 around the splice site can modulate different AS events. For that, we profiled nucleosome
 173 signals of 3032 cold-regulated DAS events that showed significant (p -value <0.05) Δ PSI values
 174 upon cold stress. Interestingly, different DAS events displayed significant changes in
 175 nucleosome occupancy signals around the donor and acceptor sites of different AS events at
 176 22°C and 4°C (One-way ANOVA-test, $p < 0.01$, Fig 2a). We also could detect an overall drop
 177 of nucleosome occupancy level for all AS events upon cold stress. For example, nucleosome
 178 occupancy is relatively higher for ES event at 22°C compared to 4°C (One-tailed t test, p
 179 <0.0001 , Fig 2a) potentially impacting exon definition and loss of exons from different
 180 transcripts (Fig. 2a). Since nucleosome occupancy levels differentially associate with various
 181 types of AS events between plants grown at different temperatures, we sought to explore if this
 182 relationship holds true to explain the ratios of these AS events. For that, we grouped PSI values
 183 (see Methods) for different AS events detected in plants grown at both temperature conditions
 184 into four bins and aligned nucleosome peaks 200 base pairs (bp) upstream and downstream the

185 exon (or intron) for which the PSI value was calculated. It is notable that for ES, A3'SS and
186 A5'SS, alternative regions with higher inclusion levels (higher PSI values) display more
187 nucleosome occupancy across the splice sites, whereas IRs with higher inclusion levels display
188 less nucleosome occupancy across the splice sites (One-way ANOVA-test, $p < 0.001$, Fig 2.b).
189 Collectively, the differences in nucleosome occupancy levels detected for plants grown at
190 different temperatures for different AS events or for the same PSI group within the same AS
191 event show that alternative regions involved in different types of AS events may be associated
192 with specific epigenetic features potentially influencing local splicing events and abundance of
193 transcripts.

194 Nucleosome occupancy is strongly associated with negative or positive AS 195 regulation

196 Next, we interrogated how nucleosome occupancy levels, for the same set of genes, differ
197 between DAS and non-DAS genes under normal and cold conditions. For that, we profiled
198 nucleosome occupancy levels across the exons of DAS and non-DAS genes. We found
199 relatively lower nucleosome occupancy for DAS compared to non-DAS exons at 22°C and as
200 well as 4°C (One-tailed t test, $p < 0.0001$, Fig. 3a). Since nucleosome occupancy globally drops
201 under cold conditions, we sought to investigate how nucleosome occupancy would correlate
202 with splice junctions affected differently by cold stress. Therefore, we grouped the SJs of the
203 AS events (p -value < 0.05) obtained from SUPPA based on their Δ PSI value to obtain
204 positively, negatively, and unaffected SJs (Supporting Information Method S1). Interestingly,
205 cold stress positively regulates 1208 SJs, negatively regulates 1054, and leaves 673 SJs un-
206 affected. (Fig. 3b; Table S7), This data strongly supports previous data showing that cold-stress
207 induced AS in plants (Calixto *et al.*, 2018). To profile nucleosome occupancy around these SJs,
208 we plotted nucleosome density of negatively-, positively-affected, and unaffected SJs for Col-0
209 grown at 22°C and 4°C (Fig. 3c). Remarkably, nucleosome profiles of unaffected SJs for both,
210 the donor and acceptor site are significantly different compared to negatively or positively
211 affected SJs at both temperatures (One-way ANOVA, $p < 0.01$, Fig. 3C). Additionally, we also
212 detected a significant association between negatively and positively affected SJs with regions
213 associated with DNPs (Fisher exact test, p -value < 0.001). Overall, our results show that
214 changes in nucleosome occupancy levels across intron-exon junctions and exons are likely to
215 regulate splice site selection and subsequently modulate splicing regulation in both positive
216 and negative manner.

217

218 **Characteristic nucleosome occupancy patterns define exons**

219 EIs have a lower guanine-cytosine (GC) content than adjacent sequences of EI-containing
220 exons (Marquez *et al.*, 2015). Therefore, we asked whether differential GC content in EI
221 sequences is associated with nucleosome occupancy to distinguish them from flanking exonic
222 regions. To answer this, we profiled nucleosome occupancy across ~2400 EIs identified in
223 Arabidopsis (Marquez *et al.*, 2015; Zhang *et al.*, 2017) and 500 bp upstream and downstream
224 from their starts and ends. We found sharp peaks of nucleosome occupancy located before the
225 start and after the end of EIs and slightly lower occupancy in the middle of EIs, which is
226 different from nucleosome patterns observed across exons (Fig. S3). Additionally, we detected
227 a decrease of nucleosome occupancy across exons under cold stress (One-tailed *t* test, p
228 <0.0001 , Fig. 4a). Comparison of nucleosome occupancy levels over EIs grouped into four
229 bins according to the PSI values showed that higher exon inclusion correlates with higher
230 nucleosome occupancy and showed variable levels under normal and cold conditions (Fig. 4b),
231 hence pointing towards their regulation under cold stress. This pattern differs from the one
232 observed for IRs, where IRs with higher inclusion levels display less nucleosome occupancy
233 (Fig. 2b). Interestingly, in this respect, EIs are more similar to ES, A5'SS and A3'SS events
234 due to their exonic features (Fig. 2b). Since EIs have a higher GC content than IRs and
235 constitutive introns (Marquez *et al.*, 2015), we compared their nucleosome profiles in normal
236 and cold conditions. We observed that nucleosome occupancy levels are higher for EIs
237 compared to IRs at 22°C and 4°C (One-way ANOVA, $p <0.0001$, Fig. 4c). This implies that
238 chromatin structure plays different roles in the definition and splicing of IRs and EIs. Overall,
239 these results revealed the importance of nucleosome occupancy in defining EIs and their
240 distinction from IRs to regulate their AS profiles under normal and cold conditions.

241

242 **Discussion**

243 Recent evidence from Arabidopsis shows that transcription and splicing are largely coupled
244 (Dolata *et al.*, 2015; Hetzel *et al.*, 2016; Ullah *et al.*, 2018; Jabre *et al.*, 2019; Jia *et al.*, 2020),
245 and that epigenetic features in plants regulate transcriptional activity and differentially mark
246 exons and introns (Zhu *et al.*, 2018). Not surprisingly, very recent studies employing
247 sequencing of chromatin-bound RNAs reveal that almost all introns in Arabidopsis are spliced

248 co-transcriptionally (Li *et al.*, 2020). Furthermore, RNAPII elongation speed has been found
249 to be slower in nucleosome-rich exons allowing more time for the splicing process to take place
250 (Chodavarapu *et al.*, 2010; Zhu *et al.*, 2018). However, how the chromatin environment
251 influences different types of AS events and their ratios under variable growth and stress
252 conditions remains elusive in plants. Since splicing/AS regulation is achieved by the context
253 of the *cis*-regulatory sequences as well as the chromatin environment (Reddy *et al.*, 2013), it is
254 important to understand the relative contributions of epigenetic landscapes. In this study, using
255 Arabidopsis Col-0 ecotype plants, we demonstrate that cold-induced DAS is accompanied by
256 changes in nucleosome occupancy levels. Although nucleosome occupancy falls globally
257 under cold conditions in Arabidopsis; nonetheless, nucleosome profiles around intron/exon
258 boundaries among different PSI groups, negatively and positively affected AS events displayed
259 characteristic patterns. Further work is needed to understand how variable nucleosome
260 occupancy modulates RNAPII processivity and alternative splicing in plants. However, since
261 nucleosome occupancy and RNAPII density has a close relationship in Arabidopsis
262 (Chodavarapu *et al.*, 2010), it is likely that chromatin architecture plays a similar role in plants
263 and animals as progesterone treated breast cancer cells displayed weaker nucleosome densities
264 and lower RNAPII accumulation, resulting in alteration in splice site recognition and exon
265 skipping (Iannone *et al.*, 2015). Since histone modification modulate AS in humans (Luco *et al.*
266 *et al.*, 2010), similar mechanism also may modulate splicing variation in plants. Intriguingly,
267 exons also show distinctive nucleosome occupancy (Fig. 4), which may help to differentiate
268 them from flanking exonic regions. Furthermore, despite their classification as a group of IR,
269 exons display different nucleosome patterns compared to retained introns; pointing to their
270 distinct regulation.

271 We propose that these changes in nucleosome occupancy may provide the basic definition to
272 exons and introns to coordinate RNAPII processivity. However, it is apparent that the splicing
273 process is also fine-tuned by various *trans*-regulatory factors and histone modifications under
274 variable growth and stress conditions (Kindgren *et al.*, 2019; Zhu *et al.*, 2020). Our data support
275 this notion and it is likely that higher nucleosome occupancy may regulate RNAPII
276 accumulation around splice sites and enable SFs recruitment to facilitate and/or modulate
277 splicing variation. Interestingly, RNAPII elongation speed in Arabidopsis would be much
278 slower after clearing a 3'SS and towards the end of an exon, and may not provide sufficient
279 time (because of higher speed in plant introns) for RNAPII to recognise the 5'SS (Kindgren *et al.*
280 *et al.*, 2019). Furthermore, recent findings show that RNAPII accumulates upstream of the 5'SS,

281 potentially to provide additional time/checkpoint to regulate splicing in mammals and plants
282 (Kindgren *et al.*, 2019; Nojima *et al.*, 2015). Therefore, variation in nucleosome occupancy
283 with an additional peak just after 5'SS (Fig. 3a) may mediate RNAPII accumulation and
284 influence CTS (Nojima *et al.*, 2015; Kindgren *et al.*, 2019). Arguably, this is why 5'SS splicing
285 dynamics are much more complicated and the scanning splicing machinery has to travel to the
286 branch point/ polypyrimidine tract to complete lariat formation and process 5'SS. Beggs and
287 colleagues proposed, the initial propensity of splicing is low but increases subsequently to
288 allow accumulation of splicing precursors to improve splicing efficiency in subsequent and/or
289 successive reactions (Aitken *et al.*, 2011). These findings are in broad agreement with CTS in
290 Arabidopsis as the CTS process is more efficient in genes with multiple introns/exons and is
291 independent of the gene length (Zhu *et al.*, 2020). Mutations at the 3'SS and 5'SS impact
292 transcription initiation and a mutant 3'SS reduces the first step of CTS in yeast (Aitken *et al.*,
293 2011). Similarly, splicing dynamics of the human beta-globin gene which fails to form lariat
294 formation and complete 5'SS when a deletion removes the polypyrimidine tract and AG
295 dinucleotide at the 3'SS (Reed & Maniatis, 1985). Therefore, it is tempting to speculate that
296 nucleosome occupancy and/or histone decorations may be more important in the 5' regions of
297 exons providing a checkpoint to the elongating RNAPII to help recognise 5'SS, form lariat and
298 cleave at the 5'SS and 3'SS. It is evident that efficient splicing/AS is dependent on an optimum
299 RNAPII elongation speed and any variation (slow or fast) results in changes in splicing patterns
300 in humans and plants (Dujardin *et al.*, 2014; Godoy Herz *et al.*, 2019; Leng *et al.*, 2020).

301 Collectively our data points towards the importance of epigenetic features such as nucleosome
302 occupancy for plants grown under different and recurrent growth and stress conditions.

303

304 **Funding**

305 We thank the funding agencies for research support. Leverhulme Trust [RPG-2016-014]; DOE
306 Office of Science, Office of Biological and Environmental Research (BER) [DE-
307 SC0010733]; National Science Foundation and the US Department of Agriculture (ASNR);
308 Austrian Science Fund (FWF) for MK [P26333]. Funding for open access charge: Leverhulme
309

310 **Availability of Data and Materials**

311 All RNA-Seq and MNase-Seq raw data generated in this work is submitted to NCBI-SRA
312 under the accession number "PRJNA592356".

313

314 **Supplemental Information**

315 Supplemental Information is available at New Physiologist online.

316

317 **References**318 **Aitken S, Alexander RD, Beggs JD. 2011.** Modelling reveals kinetic advantages of co-
319 transcriptional splicing. *PLoS Computational Biology* **7**: e1002215.320 **Alamancos GP, Pagès A, Trincado JL, Bellora N, Eyras E. 2015.** Leveraging transcript
321 quantification for fast computation of alternative splicing profiles. *RNA* **21**: 1521-1531.322 **Alexander RD, Innocente SA, Barrass JD, Beggs JD. 2010.** Splicing-Dependent RNA
323 polymerase pausing in yeast. *Molecular Cell* **40**: 582-593.324 **Bolger AM, Lohse M, Usadel B. 2014.** Trimmomatic: A flexible trimmer for Illumina
325 sequence data. *Bioinformatics* **30**: 2114–2120.326 **Brody Y, Neufeld N, Bieberstein N, Causse SZ, Böhnlein EM, Neugebauer KM, Darzacq
327 X, Shav-Tal Y. 2011.** The in vivo kinetics of RNA polymerase II elongation during co-
328 transcriptional splicing. *PLoS Biology* **9**: e1000573.329 **Calixto CPG, Guo W, James AB, Tzioutziou NA, Entizne JC, Panter PE, Knight H,
330 Nimmo HG, Zhang R, Brown JWS. 2018.** Rapid and dynamic alternative splicing impacts
331 the arabidopsis cold response transcriptome[CC-BY]. *Plant Cell* **30**: 1424-1444.332 **Chen W, Liu Y, Zhu S, Green CD, Wei G, Han JDJ. 2014.** Improved nucleosome-
333 positioning algorithm iNPS for accurate nucleosome positioning from sequencing data. *Nature*
334 *Communications* **18**: 4909-4923.335 **Chen K, Xi Y, Pan X, Li Z, Kaestner K, Tyler J, Dent S, He X, Li W. 2013.** DANPOS:
336 Dynamic analysis of nucleosome position and occupancy by sequencing. *Genome Research*
337 **23**: 341–351.338 **Chodavarapu RK, Feng S, Bernatavichute Y V., Chen PY, Stroud H, Yu Y, Hetzel JA,
339 Kuo F, Kim J, Cokus SJ, et al. 2010.** Relationship between nucleosome positioning and DNA
340 methylation. *Nature* **466**: 388-392.

- 341 **Dolata J, Guo Y, Kowierz A, Smolinski D, Brzyzek G, Jarmowski A, Swiezewski S.**
342 **2015.** NTR1 is required for transcription elongation checkpoints at alternative exons in
343 Arabidopsis. *The EMBO Journal* **34**: 544–558.
- 344 **Dujardin G, Lafaille C, de la Mata M, Marasco LE, Muñoz MJ, Le Jossic-Corcoss C,**
345 **Corcoss L, Kornblihtt AR. 2014.** How slow RNA Polymerase II elongation favors alternative
346 exon skipping. *Molecular Cell* **54**: 683–690.
- 347 **Filichkin SA, Hamilton M, Dharmawardhana PD, Singh SK, Sullivan C, Ben-Hur A,**
348 **Reddy ASN, Jaiswal P. 2018.** Abiotic stresses modulate landscape of poplar transcriptome
349 via alternative splicing, differential intron retention, and isoform ratio switching. *Frontiers in*
350 *Plant Science* **9**: 5-22.
- 351 **Godoy Herz MA, Kubaczka MG, Brzyzek G, Servi L, Krzyszton M, Simpson C, Brown**
352 **J, Swiezewski S, Petrillo E, Kornblihtt AR. 2019.** Light regulates plant alternative splicing
353 through the control of transcriptional elongation. *Molecular Cell* **73**: 1066-1074.
- 354 **Hetzel J, Duttke SH, Benner C, Chory J. 2016.** Nascent RNA sequencing reveals distinct
355 features in plant transcription. *Proceedings of the National Academy of Sciences* **113**: 12316-
356 12321.
- 357 **Huang DW, Sherman BT, Lempicki RA. 2009a.** Systematic and integrative analysis of large
358 gene lists using DAVID bioinformatics resources. *Nature Protocols* **4**: 44–57.
- 359 **Huang DW, Sherman BT, Lempicki RA. 2009b.** Bioinformatics enrichment tools: Paths
360 toward the comprehensive functional analysis of large gene lists. *Nucleic Acids Research* **37**:
361 1–13.
- 362 **Iannone C, Pohl A, Papasaikas P, Soronellas D, Vicent GP, Beato M, Valcárcel J. 2015.**
363 Relationship between nucleosome positioning and progesterone-induced alternative splicing in
364 breast cancer cells. *RNA* **21**: 360-374.
- 365 **Jabre I, Reddy ASN, Kalyna M, Chaudhary S, Khokhar W, Byrne LJ, Wilson CM, Syed**
366 **NH. 2019.** Does co-transcriptional regulation of alternative splicing mediate plant stress
367 responses? *Nucleic acids research* **47**: 2716-2726.
- 368 **Kindgren P, Ivanov M, Marquardt S. 2019.** Native elongation transcript sequencing reveals
369 temperature dependent dynamics of nascent RNAPII transcription in Arabidopsis **48**: 2332-
370 2347.

- 371 **Laloum T, Martín G, Duque P. 2017.** Alternative splicing control of abiotic stress responses.
372 *Trends in Plant Science* **23**: 140-150.
- 373 **Lämke J, Bäurle I. 2017.** Epigenetic and chromatin-based mechanisms in environmental
374 stress adaptation and stress memory in plants. *Genome Biology* **18**: 1-11.
- 375 **Langmead B, Trapnell C, Pop M, Salzberg SL. 2009.** Ultrafast and memory-efficient
376 alignment of short DNA sequences to the human genome. *Genome biology* **10**: R25.
- 377 **Leng X, Ivanov M, Kindgren P, Malik I, Thieffry A, Sandelin A, Kaplan CD, Marquardt
378 S, Plant C, Centre S, et al. 2020.** Organismal benefits of transcription speed control at gene
379 boundaries. *EMBO reports* **21**: e49315.
- 380 **Li S, Wang Y, Zhao Y, Zhao X, Chen X, Gong Z. 2020.** Global co-transcriptional splicing
381 in Arabidopsis and the correlation with splicing regulation in mature RNAs. *Molecular Plant*
382 **13**: 266-277.
- 383 **Luco RF, Pan Q, Tominaga K, Blencowe BJ, Pereira-Smith OM, Misteli T. 2010.**
384 Regulation of alternative splicing by histone modifications. *Science* **327**: 996–1000.
- 385 **Marquez Y, Höpfler M, Ayatollahi Z, Barta A, Kalyna M. 2015.** Unmasking alternative
386 splicing inside protein-coding exons defines exons and their role in proteome plasticity.
387 *Genome Research* **25**: 995–1007.
- 388 **Nojima T, Gomes T, Grosso ARF, Kimura H, Dye MJ, Dhir S, Carmo-Fonseca M,
389 Proudfoot NJ. 2015.** Mammalian NET-seq reveals genome-wide nascent transcription
390 coupled to RNA processing. *Cell* **161**: 526-540.
- 391 **Nojima T, Rebelo K, Gomes T, Grosso AR, Proudfoot NJ, Carmo-Fonseca M. 2018.** RNA
392 Polymerase II Phosphorylated on CTD Serine 5 Interacts with the Spliceosome during Co-
393 transcriptional Splicing. *Molecular Cell* **72**: 369-379.
- 394 **Patro R, Duggal G, Love MI, Irizarry RA, Kingsford C. 2017.** Salmon provides fast and
395 bias-aware quantification of transcript expression. *Nature Methods* **14**: 417-419.
- 396 **Ramírez F, Dündar F, Diehl S, Grüning BA, Manke T. 2014.** DeepTools: A flexible
397 platform for exploring deep-sequencing data. *Nucleic Acids Research* **42**: W187-W191.
- 398 **Reddy ASN, Marquez Y, Kalyna M, Barta A. 2013.** Complexity of the alternative splicing
399 landscape in plants. *The Plant cell* **25**: 3657–83.

- 400 **Reed R, Maniatis T. 1985.** Intron sequences involved in lariat formation during pre-mRNA
401 splicing. *Cell* **41**: 95-105.
- 402 **Roy D, Paul A, Roy A, Ghosh R, Ganguly P, Chaudhuri S. 2014.** Differential acetylation
403 of histone H3 at the regulatory region of OsDREB1b promoter facilitates chromatin
404 remodelling and transcription activation during cold stress. *PLoS ONE* **9**: e100343.
- 405 **Sibley CR, Blazquez L, Ule J. 2016.** Lessons from non-canonical splicing. *Nature Reviews*
406 *Genetics* **17**: 407–421.
- 407 **Staiger D, Simpson GG. 2015.** Enter exitrons. *Genome Biology* **16**: 1-3.
- 408 **Tilgner H, Knowles DG, Johnson R, Davis CA, Chakraborty S, Djebali S, Curado J,**
409 **Snyder M, Gingeras TR, Guigó R. 2012.** Deep sequencing of subcellular RNA fractions
410 shows splicing to be predominantly co-transcriptional in the human genome but inefficient for
411 lncRNAs. *Genome Research* **22**: 1616–1625.
- 412 **Trincado JL, Entizne JC, Hysenaj G, Singh B, Skalic M, Elliott DJ, Eyraas E. 2018.**
413 SUPPA2: Fast, accurate, and uncertainty-aware differential splicing analysis across multiple
414 conditions. *Genome Biology* **19**: 1-11.
- 415 **Ullah F, Hamilton M, Reddy ASN, Ben-Hur A. 2018.** Exploring the relationship between
416 intron retention and chromatin accessibility in plants. *BMC Genomics* **19**: 21-32.
- 417 **Yu X, Meng X, Liu Y, Wang X, Wang TJ, Zhang A, Li N, Qi X, Liu B, Xu ZY. 2019.** The
418 chromatin remodeler ZmCHB101 impacts alternative splicing contexts in response to osmotic
419 stress. *Plant Cell Reports* **38**: 131–145.
- 420 **Zhang R, Calixto C, Marquez Y, Venhuizen P. 2016.** AtRTD2: A Reference Transcript
421 Dataset for accurate quantification of alternative splicing and expression changes in
422 *Arabidopsis thaliana* RNA-seq data. *BioRxiv*: 051938.
- 423 **Zhang R, Calixto CPG, Marquez Y, Venhuizen P, Tzioutziou NA, Guo W, Spensley M,**
424 **Entizne JC, Lewandowska D, Have S Ten, et al. 2017.** A high quality *Arabidopsis*
425 transcriptome for accurate transcript-level analysis of alternative splicing. *Nucleic Acids*
426 *Research* **45**: 5061-5073.
- 427 **Zhang Q, Oh DH, DiTusa SF, RamanaRao M V., Baisakh N, Dassanayake M, Smith AP.**
428 **2018.** Rice nucleosome patterns undergo remodeling coincident with stress-induced gene
429 expression. *BMC Genomics* **19**: 1–16.

- 430 **Zhu JK. 2016.** Abiotic stress signaling and responses in plants. *Cell* **167**: 313–324.
- 431 **Zhu J, Liu M, Liu X, Dong Z. 2018.** RNA polymerase II activity revealed by GRO-seq and
432 pNET-seq in Arabidopsis. *Nature Plants* **4**: 1112-1123.
- 433 **Zhu D, Mao F, Tian Y, Lin X, Gu L, Gu H, Qu L, Wu Y, Wu Z. 2020.** The features and
434 regulation of co-transcriptional splicing in Arabidopsis. *Molecular Plant* **13**: 278-294.

435

436

437

438

439

440

441

442

443

444

445

446

447

For Peer Review

448 Figure Legends

449 **Fig. 1** Cold-induced changes in gene expression, alternative splicing, and nucleosome
 450 occupancy. **(a)** Venn diagram displaying the overlap between DEGs and DAS genes. **(b)**
 451 Histogram representing the number of DAS events detected in Arabidopsis RNA-seq data upon
 452 cold stress. **(c)** Venn diagram displaying the overlap between DAS genes and the genes
 453 detected within the differentially positioned nucleosome regions. DEGs and DAS are
 454 differentially expressed and alternatively spliced, genes, respectively. DNPs and DNPs-Genes
 455 are differentially positioned nucleosomes and the genes associated with them, respectively. The
 456 p -value (hypergeometric test) relates to the significance of overlap. A5'SS: Alternative 5' splice
 457 site, A3'SS: Alternative 3' splice site, IR: Intron retention events without exons, MX:
 458 Mutually exclusive exons, ES: Skipped exon, AF: Alternative first exon, EI: Exitrons, and AL:
 459 Alternative last exon.

460 **Fig. 2** Association of nucleosome occupancy with different AS events and their different ratios.
 461 **(a)** The association of nucleosome occupancy with different AS events. The x-axis is the
 462 position relative to the acceptor site (left) and donor site (right); the y-axis is the average of
 463 nucleosome signal for the selected genomic regions. ANOVA-test has been performed to detect
 464 the significance of differential nucleosome occupancy around acceptor site ($p = 0.015$) and
 465 donor site ($p = 0.039$) of different AS events of Col-0 at 22°C, and the donor ($p = 0.0138$) and
 466 the acceptor sites ($p = 0.0196$) of different AS events of Col-0 at 4°C **(b)** Nucleosome profiles
 467 for different types of AS events grouped based on their PSI. ANOVA-test has been performed
 468 to detect significance of differential nucleosome occupancy of different PSI groups for of Col-
 469 0 at 22°C and 4°C, respectively; around the acceptor site of A3'SS ($p = 0.0129$, $p = 0.00112$),
 470 A5'SS ($p = 0.00033$, $p = 0.0112$), ES ($p = 0.000129$, $p = 0.00234$), and IR ($p = 0.00236$, $p =$
 471 0.132), events. The x-axis is the position relative to the acceptor site; the y-axis is the average
 472 of nucleosome signal. ES: Exon skipping, A3'SS: Alternative 3'SS, A5'SS: Alternative 5'SS,
 473 and IR: Intron retention. Constitutive exons or introns are coloured in yellow, whereas
 474 exons/introns involved in the splicing event are coloured in blue. Curved lines indicate a
 475 splicing event. Red arrow pointing towards differences in scaling used to plot nucleosome
 476 profiles for 22°C and 4°C. Blue arrows indicate regions with significant changes in nucleosome
 477 occupancy.

478 **Fig. 3** Profiles of nucleosome occupancy across DAS, non-DAS exons and alternatively spliced
 479 junctions. **(a)** Nucleosome profiles are plotted against the DAS and non-DAS exons with 500
 480 bp upstream and downstream at 22°C (left) and 4°C (right), respectively. Nucleosome signal
 481 data were used in one-tailed t test, which confirmed that DAS exons has lower nucleosome
 482 occupancy compared to non-DAS exons at 22°C and 4°C ($p = 4.31977E^{-16}$) drops across DAS
 483 exons upon temperature shift ($p = 5.32124E^{-18}$), and that nucleosome occupancy profiles
 484 around DAS exons are different between Col-0 22°C and 4°C ($p = 1.05564E^{-65}$). The x-axis
 485 represents DAS/non-DAS exons scaled to 500 bp and their upstream and downstream flanking
 486 regions (500 bp); the y-axis represents the average nucleosome signal in the selected genomic
 487 regions. **(b)** Chart illustrating the number of AS junctions that are unaffected, positively or
 488 negatively affected. Percentages are calculated relative to the significant (p -value <0.05) AS
 489 detected by SUPPA **(c)** Average nucleosome occupancy level across donor (left) and acceptor
 490 (right) regions of all splicing junctions which are unaffected, positively, or negatively affected
 491 by cold stress. One-way ANOVA test show the significance of the differences in nucleosome
 492 occupancy for the different types of SJs around the donor ($p = 0.00813$; Col-0 22°C, $p = 0.0206$;

493 Col-0 4°C) and the acceptor ($p = 0.0293$; Col-0 22°C, $p = 0.00733$, Col-0 4°C). Red arrow
 494 pointing towards differences in scaling used to plot nucleosome profiles for 22°C and 4°C. Blue
 495 arrows indicate regions with significant changes in nucleosome occupancy.

496 **Fig. 4** Nucleosome profiles across exons and their flanking regions. **(a)** Nucleosome profiles
 497 across exons and -500/+500 bp flanking regions. Nucleosome signal data collected across
 498 exons were used in one-tailed t test, which confirmed that nucleosome signal across exons
 499 drops significantly at 4°C ($p = 5.51E^{-127}$). **(b)** Nucleosome profiles for exons grouped
 500 according to their Percent Spliced In (PSI) values. The x-axis is the position relative to exons,
 501 where EIs and ELe are exon start and end, respectively; the y-axis is the average nucleosome
 502 signal. **(c)** Nucleosome occupancy across exons, retained introns, constitutively spliced
 503 introns, and their -500/+500 bp flanking regions in each sample. One-way ANOVA test has
 504 been performed to confirm the significance of the differences in nucleosome occupancy
 505 between constitutively spliced introns, exons, and IR^{-EI} at 22°C ($p = 5.99e^{-09}$) and 4°C ($p =$
 506 $1e^{-09}$). IR^{-EI} - retained introns excluding exons, S and E - start and end of exons or
 507 retained/constitutive introns. Red arrow pointing towards differences in scaling used to plot
 508 nucleosome profiles for 22°C and 4°C. Blue arrows indicate regions with significant changes
 509 in nucleosome occupancy.

510

511 Supporting Information

512 **Supporting Information Method S1** Details of the experimental procedure.

513 **Fig. S1** GO term enrichment analysis of differentially expressed genes (DEGs) and
 514 differentially alternatively spliced (DAS) genes. The x-axis represents the $-\log_{10}$ FDR
 515 (significant FDR < 0.05) value for GO term; the y-axis represents terms in biological processes
 516 (yellow), cellular components (blue), and molecular functions (green).

517 **Fig. S2** Distribution of the mean changes in Percent Spliced In (PSI) values along with the
 518 expression of different AS transcripts. The x-axis is the average transcript abundance; the y-
 519 axis is the Delta PSI (Δ PSI) detected by SUPPA. Blue and grey dots represent significant (p -
 520 value < 0.05) and non-significant events (p -value > 0.05), respectively. ASE: all splicing
 521 events; EI: exon splicing events; IR-EI: intron retention events excluding exons; IR: intron
 522 retention; A3'SS: alternative 3' splice site; A5'SS: alternative 5'SS; ES: exon skipping.

523 **Fig. S3** Genome-wide representation of nucleosome occupancy levels displaying a drop in
 524 nucleosome signal across exons and flanking regions. The x-axis represents exons scaled to
 525 500 bp and their upstream and downstream flanking regions (500 bp); the y-axis represents the
 526 average nucleosome signal level.

527 **Table S1** Differentially expressed (DE) and differentially alternatively spliced (DAS) genes
 528 identified in *Arabidopsis thaliana* upon exposure to cold stress.

529 **Table S2** Event coordinates extracted from AtRTDv2 annotation file using SUPPA as well as
 530 the percentage spliced in (PSI) of each event in different samples.

531 **Table S3** Significant (p -value ≤ 0.05) differential splicing events for local alternative splicing
 532 events (Δ PSI value) detected by SUPPA.

533 **Table S4** List of nucleosomes detected by iNPS in Col-0 at 22°C and 4°C on Chromosomes 1-
534 5.

535 **Table S5** Differential nucleosome positioning analysis performed by SUPPA and iNPS.

536 **Table S6** Genes associated with windows enriched with the differentially positioned
537 nucleosomes.

538 **Table S7** Splice Junctions (SJs) grouped into positively, negatively, and unaffected SJs.

539

For Peer Review

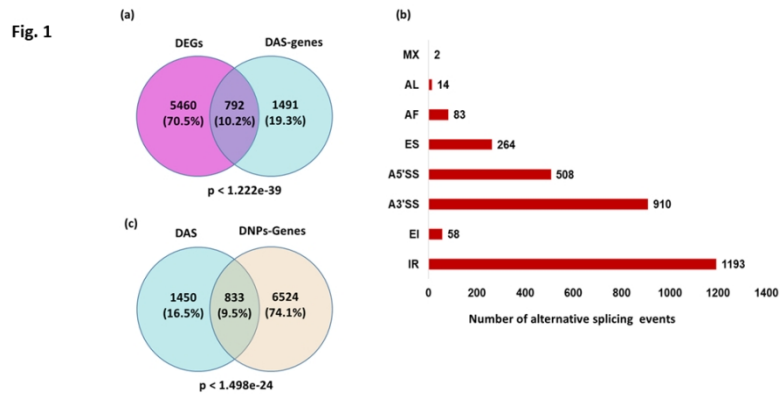


Fig. 1 Cold-induced changes in gene expression, alternative splicing, and nucleosome occupancy. (a) Venn diagram displaying the overlap between DEGs and DAS genes. (b) Histogram representing the number of DAS events detected in Arabidopsis RNA-seq data upon cold stress. (c) Venn diagram displaying the overlap between DAS genes and the genes detected within the differentially positioned nucleosome regions. DEGs and DAS are differentially expressed and alternatively spliced, genes, respectively. DNPs and DNPs-Genes are differentially positioned nucleosomes and the genes associated with them, respectively. The p-value (hypergeometric test) relates to the significance of overlap. A5'SS: Alternative 5' splice site, A3'SS: Alternative 3' splice site, IR: Intron retention events without exons, MX: Mutually exclusive exons, ES: Skipped exon, AF: Alternative first exon, EI: Exons, and AL: Alternative last exon.

338x190mm (96 x 96 DPI)

Fig. 2

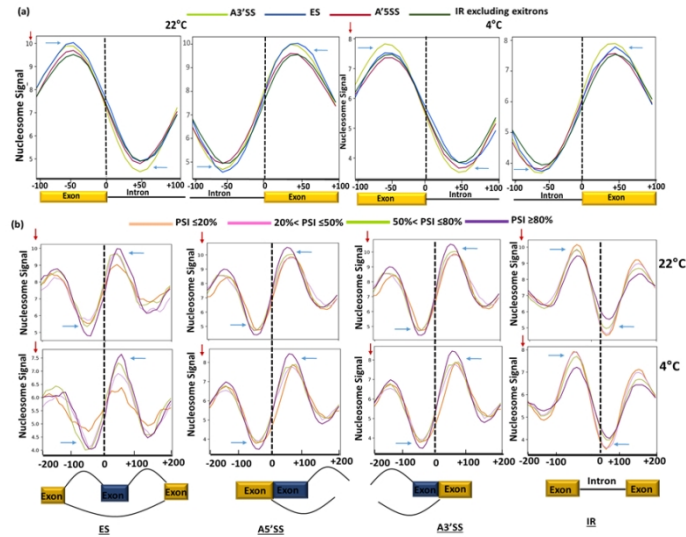


Fig. 2 Association of nucleosome occupancy with different AS events and their different ratios. (a) The association of nucleosome occupancy with different AS events. The x-axis is the position relative to the acceptor site (left) and donor site (right); the y-axis is the average of nucleosome signal for the selected genomic regions. ANOVA-test has been performed to detect the significance of differential nucleosome occupancy around acceptor site ($p = 0.015$) and donor site ($p = 0.039$) of different AS events of Col-0 at 22°C, and the donor ($p = 0.0138$) and the acceptor sites ($p = 0.0196$) of different AS events of Col-0 at 4°C. (b) Nucleosome profiles for different types of AS events grouped based on their PSI. ANOVA-test has been performed to detect significance of differential nucleosome occupancy of different PSI groups for Col-0 at 22°C and 4°C, respectively; around the acceptor site of A3'SS ($p = 0.0129$, $p = 0.00112$), A5'SS ($p = 0.00033$, $p = 0.0112$), ES ($p = 0.000129$, $p = 0.00234$), and IR ($p = 0.00236$, $p = 0.132$), events. The x-axis is the position relative to the acceptor site; the y-axis is the average of nucleosome signal. ES: Exon skipping, A3'SS: Alternative 3'SS, A5'SS: Alternative 5'SS, and IR: Intron retention. Constitutive exons or introns are coloured in yellow, whereas exons/introns involved in the splicing event are coloured in blue. Curved lines indicate a splicing event. Red arrow pointing towards differences in scaling used to plot nucleosome profiles for 22°C and 4°C. Blue arrows indicate regions with significant changes in nucleosome occupancy.

338x190mm (96 x 96 DPI)

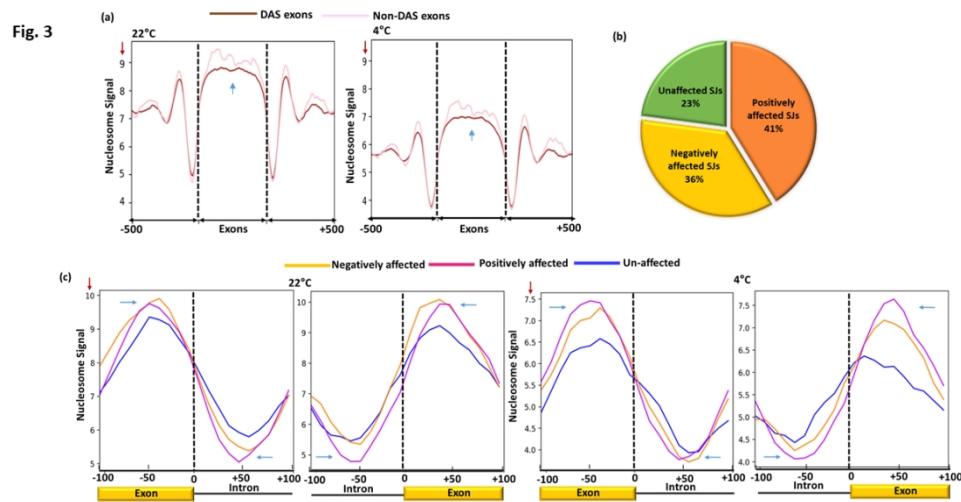


Fig. 3 Profiles of nucleosome occupancy across DAS, non-DAS exons and alternatively spliced junctions. (a) Nucleosome profiles are plotted against the DAS and non-DAS exons with 500 bp upstream and downstream at 22oC (left) and 4oC (right), respectively. Nucleosome signal data were used in one-tailed t test, which confirmed that DAS exons has lower nucleosome occupancy compared to non-DAS exons at 22oC and 4oC ($p = 4.31977E-16$) drops across DAS exons upon temperature shift ($p = 5.32124E-18$), and that nucleosome occupancy profiles around DAS exons are different between Col-0 22oC and 4oC ($p = 1.05564E-65$). The x-axis represents DAS/non-DAS exons scaled to 500 bp and their upstream and downstream flanking regions (500 bp); the y-axis represents the average nucleosome signal in the selected genomic regions. (b) Chart illustrating the number of AS junctions that are unaffected, positively or negatively affected. Percentages are calculated relative to the significant (p -value < 0.05) AS detected by SUPPA (c) Average nucleosome occupancy level across donor (left) and acceptor (right) regions of all splicing junctions which are unaffected, positively, or negatively affected by cold stress. One-way ANOVA test show the significance of the differences in nucleosome occupancy for the different types of SJs around the donor ($p = 0.00813$; Col-0 22oC, $p = 0.0206$; Col-0 4oC) and the acceptor ($p = 0.0293$; Col-0 22oC, $p = 0.00733$, Col-0 4oC). Red arrow pointing towards differences in scaling used to plot nucleosome profiles for 22oC and 4oC. Blue arrows indicate regions with significant changes in nucleosome occupancy.

338x190mm (96 x 96 DPI)

Fig. 4 Nucleosome profiles across exons and their flanking regions. (a) Nucleosome profiles across exons and -500/+500 bp flanking regions. Nucleosome signal data collected across exons were used in one-tailed t test, which confirmed that nucleosome signal across exons drops significantly at 40C ($p = 5.51E-127$). (b) Nucleosome profiles for exons grouped according to their Percent Spliced In (PSI) values. The x-axis is the position relative to exons, where EIs and EIE are exon start and end, respectively; the y-axis is the average nucleosome signal. (c) Nucleosome occupancy across exons, retained introns, constitutively spliced introns, and their -500/+500 bp flanking regions in each sample. One-way ANOVA test has been performed to confirm the significance of the differences in nucleosome occupancy between constitutively spliced introns, exons, and IR-EI at 22oC ($p = 5.99e-09$) and 40C ($p = 1e-09$). IR-EI - retained introns excluding exons, S and E - start and end of exons or retained/constitutive introns. Red arrow pointing towards differences in scaling used to plot nucleosome profiles for 22oC and 40C. Blue arrows indicate regions with significant changes in nucleosome occupancy.

338x190mm (96 x 96 DPI)